Journal of Power Sources 228 (2013) 250–255

Contents lists available at SciVerse ScienceDirect

Journal of Power Sources

journal homepage: www.elsevier.com/locate/jpowsour

A rechargeable lithium–air battery using a lithium ion-conducting lanthanum lithium titanate ceramics as an electrolyte separator

Yoshiyuki Inaguma [a,*], Mamoru Nakashima [b]

[a] Department of Chemistry, Faculty of Science, Gakushuin University, 1-5-1 Mejiro, Toshima-ku, Tokyo 171-8588, Japan
[b] Toho Titanium Co., Ltd, 3-3-5 Chigasaki, Chigasaki City, Kanagawa 253-8510, Japan

HIGHLIGHTS

- The perovskite-type $La_{2/3-x}Li_{3x}TiO_3$ (LLTO) ceramics electrolytes was prepared.
- LLTO ceramics exhibits the high total lithium ion conductivity of $3–5 \times 10^{-4}$ S cm^{-1} at 300 K.
- Using a LLTO electrolyte as a separator, a rechargeable aqueous-type lithium–air battery was successfully developed.
- The stable charge/discharge behaviors of the lithium–air battery were confirmed.

ARTICLE INFO

Article history:
Received 30 August 2012
Received in revised form
23 October 2012
Accepted 24 November 2012
Available online 29 November 2012

Keywords:
Li–air battery
Solid state electrolyte
Lithium ion conductivity
Lanthanum lithium titanate
Perovskite
Separator

ABSTRACT

We successfully prepared the perovskite-type lanthanum lithium titanate (LLTO) ceramics electrolytes with high total lithium ion conductivity of $3–5 \times 10^{-4}$ S cm^{-1} at 300 K. The high total conductivity is attributed to the elimination of resistive grain boundary by the grain growth. Using the electrolyte as a separator, a rechargeable aqueous-type lithium/air cell which composed of Li metal/Li organic electrolytes/LLTO ceramics tube/LiOH aq/O_2 carbon electrodes was developed and the stable discharge/charge behaviors were confirmed. Owing to the low porosity and the stability to alkaline aqueous solution of LiOH as well as high ionic conductivity, the lithium ion-conducting lanthanum lithium titanate ceramics is suitable for an electrolyte separator for aqueous-type rechargeable lithium/air batteries.

1. Introduction

Li–air batteries have attracted significant interests based on their potentially high specific energy, which leads to the technological application of long-range electric vehicles as well as grid energy storage and potable electronics [1–4]. Since the Abraham and Jiang reported a non-aqueous polymer electrolyte-based rechargeable Li–air battery [5], Li–air batteries have been extensively studied to improve their performance and elucidate the mechanism (There are many papers regarding Li–air batteries. Please see the references cited in Ref. [1–4].). Among them, Visco et al. [6] have proposed a lithium anode protected by a lithium ion–conducting NASICON-type solid electrolyte. The aqueous type Li–air batteries based on the concept of the protected lithium anode proposed by Visco et al. have recently attracted much attention because of their advantage that the discharge reaction product such as LiOH is soluble in water. Imanishi et al. successfully fabricated rechargeable Li–air batteries with an aqueous electrolyte separated by a water stable lithium conducting glass ceramics [4,7–9]. More recently, Wang and Zhou developed a lithium–air battery with organic electrolytes and aqueous electrolyte separated by a lithium super ionic conductor film [10,11]. In all above cases, the solid electrolytes based on NASICON-type lithium ion conductors were used as a separator and other materials have not been reported.

We then propose a lithium ion-conducting perovskite as an electrolyte separator of aqueous type Li–air batteries. Lithium ion-conducting perovskites have been first reported by Latie et al. [12] on $La_{1/3}Li_xNb_{1-x}Ti_xO_3$ and Belous et al. [13,14] on $La_{2/3-x}Li_{3x}TiO_3$. Since it was found that a perovskite lanthanum lithium titanate shows lithium ion conductivity as high as 10^{-3} S cm^{-1} at room temperature [15], much attention has been paid to lithium ion conducting perovskites owing to their high bulk conductivity and

* Corresponding author. Tel.: +81 3 3986 0221x6490; fax +81 3 5992 1029.
E-mail address: yoshiyuki.inaguma@gakushuin.ac.jp (Y. Inaguma).

0378-7753/$ – see front matter © 2012 Elsevier B.V. All rights reserved.
http://dx.doi.org/10.1016/j.jpowsour.2012.11.098

the fundamental studies and studies for application as solid electrolytes have been extensively performed (There are also many references regarding the perovskite-type lithium ion-conducting oxides. Please see the review articles [16–18] and the references cited herein.). However, it has been considered that the perovskite-type lithium ion-conducting oxides such as lanthanum lithium titanates are not suitable for solid electrolytes of lithium batteries because of the low reduction-proof against lithium metal. For example, lanthanum lithium titanates react with Li metal and the reduction of Ti accompanied by lithium insertion serves to exhibit the electronic conductivity [15]. Furthermore, in spite of their high bulk (intra-grain) ionic conductivity of $\sim 10^{-3}$ S cm^{-1}, the total conductivity was not more than 1×10^{-4} S cm^{-1} [15,19,20] due to the high resistive grain boundary. This is one of primarily reasons that the application as electrolytes has not been enough developed.

In this paper we report the enhancement of the total ion-conductivity of a perovskite-type lanthanum lithium titanate electrolyte ceramics and demonstrate rechargeable aqueous type Li–air batteries using the ceramics tube as an electrolyte separator.

2. Experimental procedure

A perovskite-type lanthanum lithium titanate (LLTO) with the nominal composition of $La_{0.57}Li_{0.29}TiO_3$ ($La_{2/3-x}Li_{3x}TiO_3$ ($3x = 0.29$)). was synthesized by a solid state reaction using starting materials of La_2O_3,(>99.99%) Li_2CO_3 (>99.2%) and TiO_2 (>99.99%) powders. The 7.5% stoichiometric excess amount of Li_2CO_3 was then used considering the vaporization of Li during a high temperature treatment. The mixture of starting materials was calcined at 1150 °C for 2 h in air. The calcined powder was pressed into a plate or a tube closed at one end, which was pre-sintered at 1100 °C for 2 h and sintered at 1400–1460 °C for 6–9 h.

The phase identification was performed by a powder X-ray diffraction using a Rigaku RINT-2100 X-ray diffractometer or a PANalytical X'Pert-ProMPD X-ray diffractometer equipped a graphite monochrometer. The metal contents for La and Li were determined using an inductive coupled plasma atomic emission spectroscopy (ICP-AES). The content of Ti was determined by the volumetric titration with a standard ammonium iron (III) sulfate solution after the reduction of titanium from +4 to +3 with aluminum metal. The aqueous solution for the ICP-AES and titration was then prepared as follows: The sample powder was dissolved in the melt of NaOH and Na_2O_2 in a zirconium crucible and cooled to room temperature, followed by an addition of water and conc. HCl aqueous solution. The surface of sintered samples was observed by a Hitachi S-4700 field-emission scanning electron microscopy (SEM). The average grain size of the sintered sample was measured using a Mountech Mac-View (Ver. 4) particle size distribution analysis software. The grain size was then defined as the long side of the minimum rectangle surrounding a grain and the grain size of 300 grains was averaged. Furthermore, in order to evaluate the strength of LLTO ceramics sintered at 1450 °C, the bending strength of specimen with the size of 35 mm × 4.0 mm × 3.0 mm was measured.

The lithium ion conductivity of LLTO ceramics was measured by an ac impedance method using a HP 4192A in the frequency range of 5 Hz–13 MHz. The surface of sintered plate was polished using #150 and #600 diamond laps prior to the impedance measurement. The detail of electrodes for measurement will be described in the next section.

Using a LLTO ceramics tube closed at one end as an electrolyte separator, the aqueous-type lithium–air battery was fabricated. Fig. 1 shows the schematics of fabricated lithium–air battery using a SUS container. The organic electrolyte (1.0 M $LiClO_4$ in 1:1 ethylene carbonate (EC)/dimethyl carbonate (DMC)) in which the Li metal anode was placed, was separated by the LLTO ceramics tube with

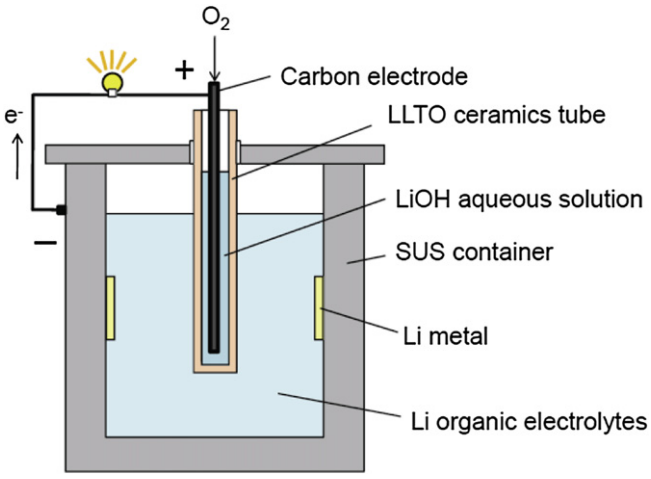

Fig. 1. A schematic representation of a rechargeable Li–air battery using LLTO as an electrolyte separator.

a thickness of 2 mm from an aqueous electrolyte (LiOH aqueous solution with an initial concentration of 0.5 M). A porous carbon tube electrode closed at one end was placed in the LiOH aqueous solution. Oxygen gas (>99.5% in purity) of 100 mL min^{-1} was flowed into the carbon electrode. The electrochemical measurements were performed using a HOKUTO DENKO HJ1001SD8 battery charge/discharge unit.

3. Results and discussion

Fig. 2 shows the powder X-ray diffraction pattern of LLTO ceramics sintered at 1450 °C. The main phase was crystallized into an orthorhombic perovskite (space group: *Cmmm*) with the lattice parameters: $a = 0.7737(1)$ nm, $b = 0.7742(1)$ nm, $c = 0.7785(1)$ nm, which corresponds to the cell $\sim 2a_p \times \sim 2a_p \times \sim 2a_p$ (a_p is a lattice parameter of primitive perovskite cell) [21]. The small amount of rutile TiO_2 and unknown phases was observed. As no impurity phases were observed in the calcined powder at 1150 °C for 2 h, the TiO_2 phase must be produced during the sintering process. The average metal composition of sintered sample was determined to La:Li:Ti = 0.57:0.29:1, which is consistent with the nominal composition.

The relative density of LLTO ceramics plate sintered at 1400–1450 °C is greater than 96%. The bending strength of sample sintered at 1450 °C was measured to be 79 MPa. Fig. 3 shows the SEM

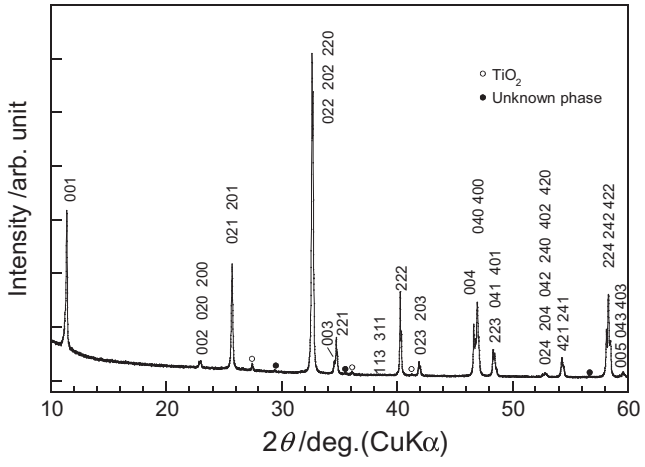

Fig. 2. Powder X-ray diffraction pattern of LLTO ceramics.

micrographs of surface for the sample sintered at 1400 °C and 1450 °C. As seen in Fig. 3, the cube-shaped particles were observed, indicating that the surface of cube-shaped particles is perpendicular to the {100} plane supposing the cubic primitive cell. The grain size of sample sintered at 1450 °C is greater than that of sample sintered at 1400 °C. The average grain size of sample sintered at 1450 °C is 25.0 μm, while that of sample sintered at 1400 °C is 12.4 μm. In order to check the leak of ceramics sample sintered at 1450 °C, we put water inside the sample a tube closed at one end and keep it for 1 day. As the result, no leak was observed.

The lithium ion conductivity of LLTO ceramics was measured according to the following procedures. Two sheets of filter papers of 10 mm square impregnated with aqueous 1 M LiCl were placed on the both side of the sample plate of 2 mm in thickness, which was sandwiched by the electrodes made from stainless steel pellet. Here, the paper impregnated with LiCl aqueous solution was used as an electrolyte in order to make clear the contribution of the grain boundary of sample. Fig. 4(a) shows the impedance plot of sintered plate of LLTO at 300 K. As seen in Fig. 4(a), two semicircles were observed with a spike. One semicircle in the higher frequency region corresponds to the contribution from the bulk part (intra-grain) and the other one in the lower frequency region corresponds to the grain boundary contribution. From the impedance plot, the lithium ion conductivity of bulk part (σ_{bulk}) was estimated to 1.6×10^{-3} S cm^{-1} at 300 K, which is consistent with previously reported data. The total lithium ion conductivity (σ_{total}) was calculated to be 5.2×10^{-4} S cm^{-1} from the sum of intra-grain and grain boundary resistances. The maximum σ_{total} was 5.7×10^{-4} S cm^{-1} at 300 K, which is the highest value among the reported data on LLTO ceramics. The activation energy for total ionic conductivity was estimated to be 0.45 eV (43 kJ mol^{-1}) from the conductivity data at 300–333 K. Next we checked the lithium ion conductivity using Li electrodes. As mentioned before, lanthanum lithium titanate reacts with Li metal and the accompanying lithium insertion leads to the electronic conductivity. In order to avoid the contact of the sample with Li, two sheets of polypropylene separator impregnated with an organic electrolyte (1 M $LiClO_4$ EC/DMC) were placed on the both side of the sample plate, which was sandwiched by Li electrodes [15]. The impedance plot at 300 K using the Li electrode was given in Fig. 4(b). As seen in Fig. 4(b), the two semicircles were clearly observed. From the impedance plot, σ_{bulk} and σ_{total} at 300 K were estimated to 1.6×10^{-3} S cm^{-1} and 3.6×10^{-4} S cm^{-1}, respectively. These values are consistent with the σ_{bulk} and σ_{total} at 300 K estimated from the impedance plot of Fig. 4(a), 1.6×10^{-3} S cm^{-1} and 5.2×10^{-4} S cm^{-1}, respectively.

The sintering temperature distinctly influenced the total ionic conductivity. The σ_{total} of samples sintered at 1400 °C and 1450 °C shown in Fig. 3 are 2.4×10^{-4} S cm^{-1} and 5.0×10^{-4} S cm^{-1}, respectively. On the other hand, the σ_{bulk} are almost the same, 1.5–1.6×10^{-3} S cm^{-1}. Therefore, the higher σ_{total} sintered at 1450 °C is attributed to the elimination of resistive grain-boundary by the grain growth.

In order to examine the water stability of LLTO, the ionic conductivity was measured after immersion for 4 weeks in deionized water or an aqueous 0.5 M LiOH. By immersion in deionized water, the σ_{bulk} and σ_{total} decreased from 1.7×10^{-3} to 1.3×10^{-3} S cm^{-1} and from 5.2×10^{-4} to 3.3×10^{-4} S cm^{-1}, respectively. Bhuvanesh et al. [22] reported that H^+/Li^+ exchange in LLTO occurred in dilute HNO_3 at 60 °C and then the lithium ion conductivity depressed. Even in deionized water a small amount of lithium ions in the sample may be substituted by protons, resulting

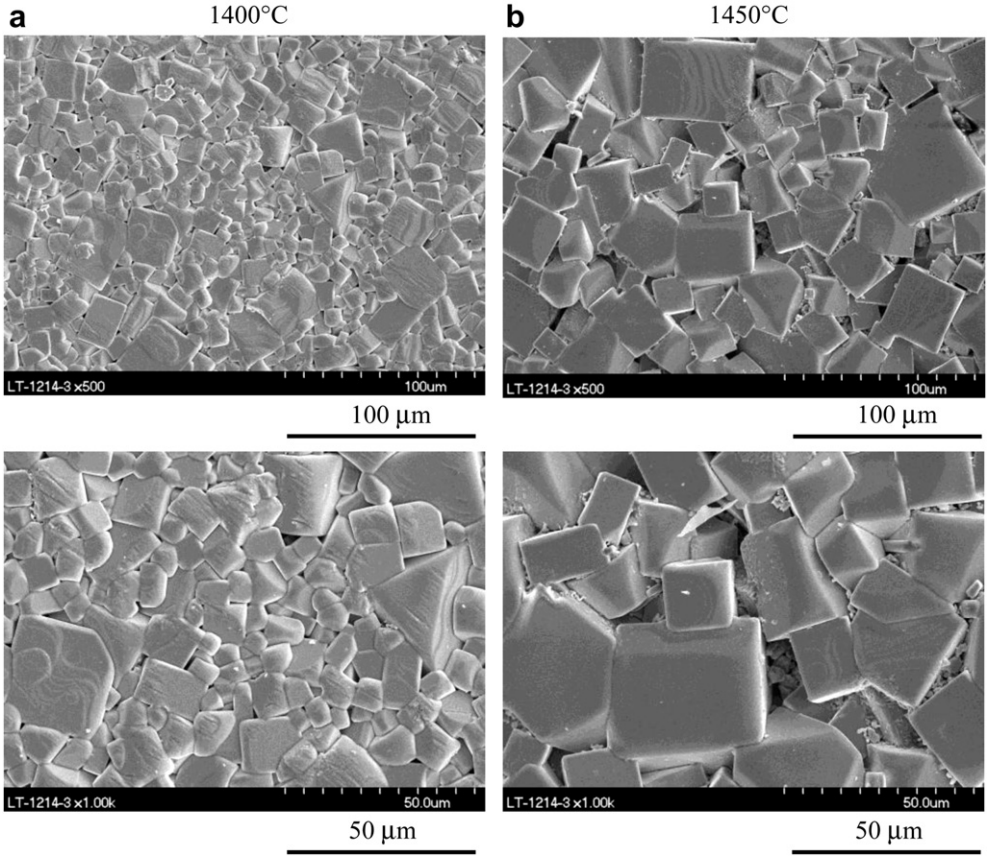

Fig. 3. SEM diagram of LLTO ceramics sintered at 1400 °C (a) and 1450 °C (b) for 6 h. The photos at the bottom are the enlarged one from the part of the ones at the top.

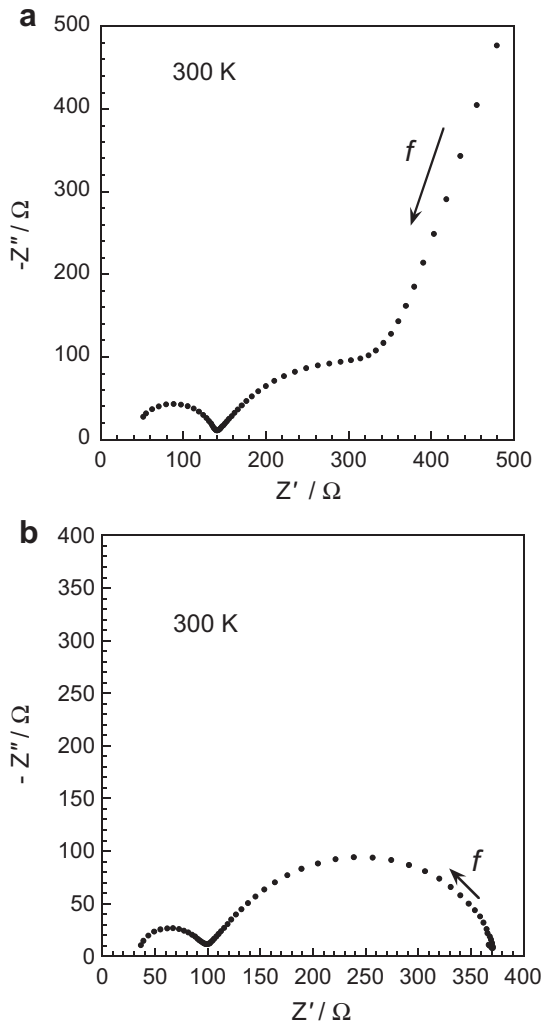

Fig. 4. Impedance plots of LLTO ceramics sintered at 1450 °C measured using the aqueous electrolyte of LiCl (a) and Li electrodes (b) at 300 K.

in the decrease in ionic conductivity. On the other hand, by immersion in an aqueous 0.5 M LiOH (pH = 12.5), the σ_{bulk} and σ_{total} did not decreased very much; from 1.6×10^{-3} to 1.5×10^{-3} S cm^{-1} and from 5.0×10^{-4} to 4.6×10^{-4} S cm^{-1}, respectively. These results imply that high pH would prevent the substitution of proton for Li ion in LLTO. Consequently LLTO ceramics is more stable in LiOH aqueous solution than in deionized water. The change in weight after immersion in both of deionized water and LiOH aqueous solution was within 0.12%. Imanishi et al. [8] have examined the water stability of NASICON-type glass ceramics Li electrolyte for aqueous-type Li/air batteries, and reported that the electrolyte is unstable in aqueous 1 M LiOH after immersion during 3 months. Our finding indicates that LLTO is a candidate of electrolyte usable in aqueous LiOH though the test duration was not enough and the concentration dependence of LiOH was not examined.

The discharge/charge properties of a fabricated Li–air cell as shown in Fig. 1 were examined. The reactions for aqueous Li–air batteries are summarized as follows:

$$\text{Positive electrode: } O_2 + 2H_2O + 4e^- \leftrightarrow 4OH^- \quad (1)$$

$$\text{Negative electrode: } Li \leftrightarrow Li^+ + e^- \quad (2)$$

$$\text{The over cell reaction: } 4Li + O_2 + 2H_2O \leftrightarrow 4LiOH \quad (3)$$

The open circuit voltage was 3.1–3.2 V, which is slightly lower than the theoretical voltage (3.51 V) supposing that the pH in aqueous LiOH is 13. Fig. 5 shows the discharge curve at a current of 1 mA for 245 h. The current density corresponding to the discharge current of 1 mA is 0.06 mA cm^{-2}, when the current density is defined as the discharge currents per the cathode area (16 cm^2). During the discharge, the operating cell voltage is stable at approximately 2.9 V. The stability in cell voltage also indicates that LLTO ceramics is chemically and electrochemically stable against LiOH solution and an organic electrolyte (1 M $LiClO_4$ EC/DMC) in the week range. Here, the concentration of LiOH in aqueous solution after the discharge for 245 h is estimated to be 1 M. Fig. 6 shows the discharge curve at the different current. Here the current densities corresponding to the various discharge currents, 1, 5, 10 and 25 mA are 0.06, 0.31, 0.63 and 1.6 mA cm^{-2}, respectively. As seen in Fig. 6, the cell voltage decreased as the current increased due to the internal resistance. The internal resistance was estimated to be 88 ± 4 Ω from the linear relationship between cell voltage and current. On the other hand, the resistance of LLTO ceramics tube with a thickness of 2 mm can be estimated to be in the range 10–20 Ω using the total conductivity. This indicates that the resistance attributable to the electrochemical reaction or the charge transfer at the surface or interface is predominant on the internal resistance. The discharge/charge curve at constant current of 1 mA was shown in Fig. 7. The same behavior was observed in repeated cycles. The charge curve at a constant current of 1 mA without O_2 gas flow was shown in Fig. S1 in the Supporting information. The saturated cell voltage (~3.9 V) is almost the same as that with the O_2 flow though the behavior of increment is different. The high overpotential in the charge process was observed for both cases. Imanishi et al. [9] successfully suppressed the overpotential during charge by employing an appropriate catalyst for air electrode and raising temperature. It is thought that the high overpotential is primarily attributed to the high activation energy for the evolution of O_2 on the carbon electrode because no catalyst for air electrode was employed. In order to confirm the produce of Li metal during charge and consumption of Li metal during discharge, the charge/discharge experiment was performed without using a lithium metal electrode initially. Fig. 8 shows the charge/discharge curve at a constant current of 2 mA of the lithium–air battery during 5 cycles without using a lithium metal electrode initially. The duration of charge was 4 h and the cut off voltage during discharge was 0.5 V. Here, the reference electrode was not independently

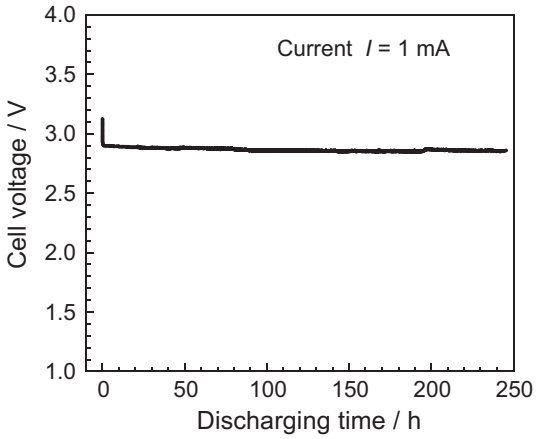

Fig. 5. Discharge curve of the lithium–air battery using LLTO as a separator at a constant current of 1 mA. The current density corresponding to the discharge current of 1 mA is 0.06 mA cm^{-2}, when the current density is defined as the discharge currents per the cathode area.

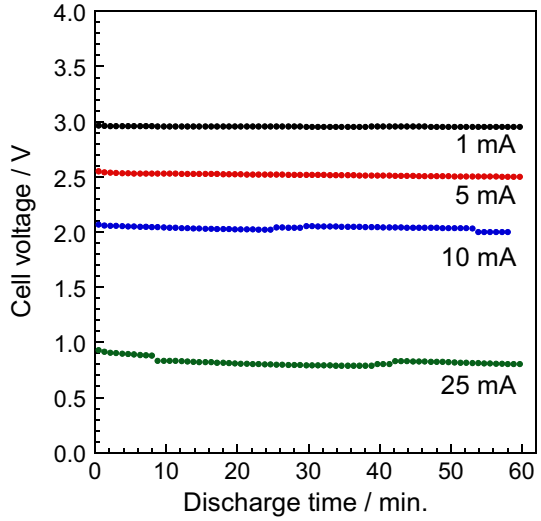

Fig. 6. Discharge curve of the lithium–air battery using LLTO as a separator at various currents of 1, 5, 10, and 25 mA. The current densities corresponding to the discharge currents, 1, 5, 10 and 25 mA are 0.06, 0.31, 0.63 and 1.6 mA cm^{-2}, respectively, when the current density is defined as the discharge currents per the cathode area.

employed. When Li metal is deposited on the surface of SUS container, the cell voltage corresponds to the voltage of carbon electrode versus the Li metal. Otherwise, the cell voltage is the voltage of carbon electrode versus the SUS. As seen in Fig. 8, in the discharge process, the cell voltage suddenly decreased after it was stable to be approximately 2.7 V, which corresponds to the consumption of Li metal produced during the charge. In addition, the stable cycling was confirmed. The findings indicate that the electrochemical reactions mentioned above occurs properly during the charge and discharge process.

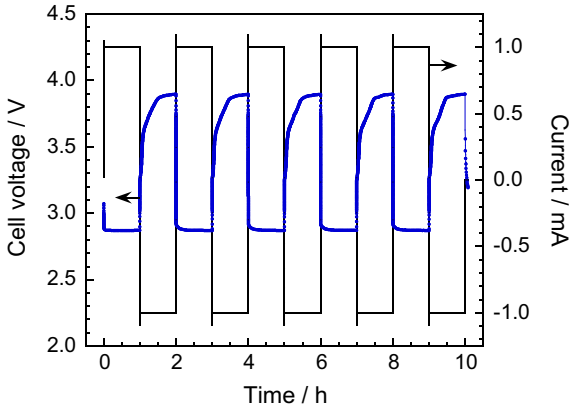

Fig. 7. Discharge/charge curve at a constant current of 1 mA of the lithium–air battery using LLTO as a separator.

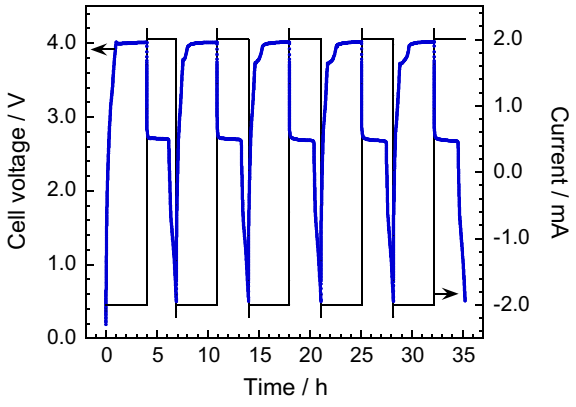

Fig. 8. Charge/discharge curve at a constant current of 2 mA of the lithium–air battery using LLTO as a separator when a lithium metal electrode was not employed initially.

In this study, we have not enough examined the long-term stability of LLTO ceramics which is the vital issue to be concerned for the application to batteries. We will elucidate and report it in the future. Furthermore, we have not optimized the air electrode materials in terms of catalytic properties. The further elucidation and optimization of air electrode materials would decrease the internal resistance and make the discharge/charge properties much better.

4. Conclusion

The perovskite-type lanthanum lithium titanate ceramics electrolytes exhibiting the high total lithium ion conductivity of 3–5 $\times$ 10^{-4} S cm^{-1} at 300 K were obtained. The high conductivity is attributed to the elimination of resistive grain-boundary by the grain growth. Using the electrolyte as a separator, a rechargeable aqueous-type lithium/air cell was fabricated and the stable discharge/charge behavior was observed. In addition, the chemical stability to alkaline LiOH aqueous solution was confirmed in the week range. Consequently, it was found that LLTO ceramics is a new candidate for the electrolyte separator for aqueous-type rechargeable lithium/air batteries. The long-term stability of LLTO ceramics against organic electrolyte and aqueous solution, and the clarification and elimination of internal resistance attributable to the interface reaction and charge transfer as well as the grain boundary resistance of LLTO ceramics are vital future issues on the development of the Li/air batteries with higher energy density. Therefore the researches for anode and cathode materials as well as electrolytes are indispensable.

Acknowledgments

Y. I. thanks Miss K. Tanaka and Dr. D. Mori for the help of powder X-ray diffraction experiments. This work was partially supported by a promotional project for the Development of Strategic Research base for private universities, and a matching fund subsidy from the Ministry of Education, Culture, Sports, Science and Technology, Japan.

Appendix A. Supplementary data

Supplementary data related to this article can be found at http://dx.doi.org/10.1016/j.jpowsour.2012.11.098.

References

[1] J. Christensen, P. Albertus, R.S. Sanchez-Carrera, T. Lohmann, B. Kozinsky, R. Liedtke, J. Ahmed, A. Kojic, J. Electrochem. Soc. 159 (2012) R1–R30.
[2] A. Kraytsberg, Y. Ein-Eli, J. Power Sources 196 (2011) 886–893.
[3] D. Capsoni, M. Bini, S. Ferrari, E. Quartarone, P. Mustarelli, J. Power Sources 220 (2012) 253–263.
[4] N. Imanishi, Y. Takeda, O. Yamamoto, Electrochemistry 80 (2012) 706–715.
[5] K.M. Abraham, Z. Jiang, J. Electrochem. Soc. 143 (1996) 1–5.
[6] S.J. Visco, E. Nimon, B. Katz, L.C.D. Jonghe, M.Y.Chu, The 12th International Meeting, Jpn. Abstr., 2004, Abstract 53.
[7] T. Zhang, N. Imanishi, S. Hasegawa, A. Hirano, J. Xie, Y. Takeda, O. Yamamoto, N. Sammes, J. Electrochem. Soc. 155 (2008) A965–A969.
[8] S. Hasegawa, N. Imanishi, T. Zhang, J. Xie, A. Hirano, Y. Takeda, O. Yamamoto, J. Power Sources 189 (2009) 371–377.
[9] T. Zhang, N. Imanishi, Y. Shimonishi, A. Hirano, Y. Takeda, O. Yamamoto, N. Sammes, Chem. Commun. 46 (2010) 1661–1663.
[10] Y. Wang, H. Zhou, J. Power Sources 195 (2010) 358–361.
[11] H. Zhou, Y. Wang, H. Li, P. He, ChemSusChem 3 (2010) 1009–1019.

[12] L. Latie, G. Villeneuve, D. Conte, G. Le Flem, J. Solid State Chem. 51 (1984) 293–299.
[13] A.G. Belous, G.N. Novitskaya, S.V. Polyanetskaya, Y.I. Gornikov, Neorg. Mater. 23 (1987) 470–472 (English translation: Inorg. Mater. 23 (1987) 412–415.).
[14] A.G. Belous, G.N. Novitskaya, S.V. Polyanetskaya, Y.I. Gornikov, Zh. Neorg. Khim 32 (1987) 283–286 (English translation: Russ. J. Inorg. Chem. 32 (1987) 156–157.).
[15] Y. Inaguma, L. Chen, M. Itoh, T. Nakamura, T. Uchida, H. Ikuta, M. Wakihara, Solid State Commun. 86 (1993) 689–693.
[16] S. Stramare, V. Thangadurai, W. Weppner, Chem. Mater. 15 (2003) 3974–3990.
[17] Y. Inaguma, J. Ceram. Soc. Jpn. 114 (2006) 1103–1110.
[18] O. Bohnké, Solid State Ionics 179 (2008) 9–15.
[19] Y. Inaguma, Y. Matsui, Y.-J. Shan, M. Itoh, T. Nakamura, Solid State Ionics 79 (1995) 91–97.
[20] A. Mei, X.-L. Wang, Y.-C. Feng, S.-J. Zhao, G.-J. Li, H.-X. Geng, Y.-H. Lin, C.-W. Nan, Solid State Ionics 179 (2008) 2255–2259.
[21] Y. Inaguma, T. Katsumata, M. Itoh, Y. Morii, J. Solid State Chem. 166 (2002) 67–72.
[22] N.S.P. Bhuvanesh, O. Bohnké, H. Duroy, M.P. Crosnier-Lopez, J. Emery, J.L. Fourquet, Mater. Res. Bull. 33 (1998) 1681–1691.